

Interface interaction and wetting in the $\text{Er}_2\text{O}_3/(\text{Cu}-\text{Al})$ and $\text{Er}_2\text{O}_3/(\text{Cu}-\text{Ti})$ systems

M. Aizenshtein · S. Barzilai · N. Froumin ·
N. Frage

Received: 16 August 2007 / Accepted: 18 October 2007 / Published online: 12 December 2007
© Springer Science+Business Media, LLC 2007

Abstract The wetting behavior and metal-oxide interface interactions in the $\text{Er}_2\text{O}_3/(\text{Cu}-\text{Al})$ and $\text{Er}_2\text{O}_3/(\text{Cu}-\text{Ti})$ systems were investigated at 1,423 K in order to evaluate the compatibility of ceramic crucibles with liquid metals, containing active elements. Pure Cu does not wet Er_2O_3 ($\Theta \approx 140^\circ$) but the wettability is significantly improved by the addition of Al or Ti. It was established that Er_2O_3 reacts with Ti and Al dissolved in liquid Cu and the wettable spinel ErAlO_3 and ErTiO_3 is formed at the interface. The amount of the released Er from the substrate as a result of the reaction and the depth of the reaction zone beneath the drop are controlled by the thermodynamic properties of liquid solutions.

Introduction

Oxide ceramics such as Al_2O_3 , MgO , Y_2O_3 and Er_2O_3 are stable compounds and are often used as structural materials in the foundry industry. Nevertheless, the presence of active elements in the melt, which also form stable oxides, leads to a chemical interaction between a crucible and a liquid solution and to dissolution of the metallic component of the substrate in the melt. In order to evaluate crucible performance sessile drop wetting experiments could be used [1–4].

Wetting behavior of oxides of rare-earth elements in contact with liquid metals has been investigated by Naidich et al. [4]. Er_2O_3 was also examined at 1,423 K in contact with various melts such as: Cu, Al and Cu–Ti alloys. It was established that Al wets the Er_2O_3 substrate ($\theta = 58^\circ$), Cu does not wet it ($\theta \sim 145^\circ$); however, Ti addition to liquid Cu reduces the contact angle to about 60° . No information, which is related to the interface composition and structure, is reported. Wetting behavior of the Y_2O_3 substrate in contact with Cu–Al alloys was discussed in our previous communication [5]. It was shown that the interaction between Y_2O_3 and Al containing liquid solution leads to the formation of the YAlO_3 spinel and to Y releasing, which dissolves in the melt.

In this article, the wetting behavior and the interface interaction in the $\text{Er}_2\text{O}_3/(\text{Cu}-\text{Al})$ and $\text{Er}_2\text{O}_3/(\text{Cu}-\text{Ti})$ systems are examined.

Experimental

Er_2O_3 substrates for wetting experiments were prepared by powder metallurgy techniques. Er_2O_3 powder (99.99% purity) was isostatically pressed under 0.3 GPa. The compacted samples were first sintered in an air furnace at 1,473 K for 5 h and then hot isostatically pressed at 1,573 K under 130 MPa for 5 h. The density of the samples was 99% of the Er_2O_3 theoretical density.

Sessile drop experiments were performed at 1,423 K in a vacuum furnace ($\sim 10^{-3}$ Pa) as was described in [6]. In order to reduce the residual oxygen content in the gaseous phase, a Ti getter was used. The surface of the substrates was polished down to 1 μm diamond paste (the measured substrate roughness (R_a) was 0.15 μm) and cleaned ultrasonically using acetone and ethanol. The composition of

M. Aizenshtein · S. Barzilai
NRC-Negev, P.O. Box 9001, Beer-Sheva 84190, Israel

S. Barzilai · N. Froumin · N. Frage (✉)
Department of Material Engineering, Ben-Gurion University,
P.O. Box 653, Beer-Sheva 84105, Israel
e-mail: nfrage@bgu.ac.il

liquid drops was varied in situ by co-melting of appropriate amounts of Al, Ti and Cu. After solidification the samples were cross-sectioned and the interface was studied using XRD and SEM (EDS, WDS) analysis. In some cases, the microstructure at the interface was investigated after chemical etching using 50 vol% HNO_3 + 50 vol% H_2O solution. Auger depth profile analysis was used in order to clarify the composition of the phases, which are formed at the $\text{Er}_2\text{O}_3/(\text{Cu-Ti})$ interface. The sensitivity factor for Er was calibrated by using Er_2O_3 as a standard.

Experimental results

Wetting

The spreading kinetics and final contact angles for the $\text{Er}_2\text{O}_3/(\text{Al-Cu})$ system at 1,423 K are presented in Fig. 1. The initial contact angle for the alloys with relatively low Al contents (<26 at%) is about 130° and remains constant during 60 min of contact. For the alloys with 50 and 60 at% Al and for pure Al the contact angle decreases with time and the spreading rate increases with the increasing Al content (Fig. 1a). The final contact angle decreases with the increasing of the Al content and for pure Al the contact angle of about 40° was observed (Fig. 1b). The spreading kinetics and the final contact angles for the $\text{Er}_2\text{O}_3/(\text{Cu-Ti})$

system at 1,423 K are presented in Fig. 2. In this system the rate of spreading is very high and equilibrium contact angle was achieved already during heating up to the temperature of experiments (Fig. 2a). Ti additions to liquid Cu significantly improve wetting and non-wetting to wetting transition takes place for the alloy containing about 10 at% Ti (Fig. 2a).

Interface characterization

The $\text{Er}_2\text{O}_3/(\text{Cu-Al})$ system

The microstructures of the interface between the Er_2O_3 substrate and Cu-Al drops with various Al content are presented in Fig. 3. The formation of the crater at the interface, which depth increases with the increasing of Al content, is clearly detected. According to the EDS analysis, the craters beneath the drops contain Cu and the ErAlO_3 phase, while the solidified drop consists of metallic matrix and dendrite-like Al_3Er intermetallic inclusions. The pure Al drop in contact with Er_2O_3 , which was detached from the substrate after solidification, was subjected to XRD analysis (Fig. 4). The X-ray pattern confirms the presence of the Al_3Er intermetallic and ErAlO_3 phases.

The interface region of the $\text{Er}_2\text{O}_3/(\text{Cu-50at}\% \text{Al})$ sample was etched in order to clarify its microstructure (Fig. 5).

Fig. 1 Spreading kinetics of various Cu-Al drops on the Er_2O_3 substrate (a) and final contact angles in the $\text{Er}_2\text{O}_3/(\text{Al-Cu})$ system as a function of the melt composition after 60 min of contact at 1,423 K (b)

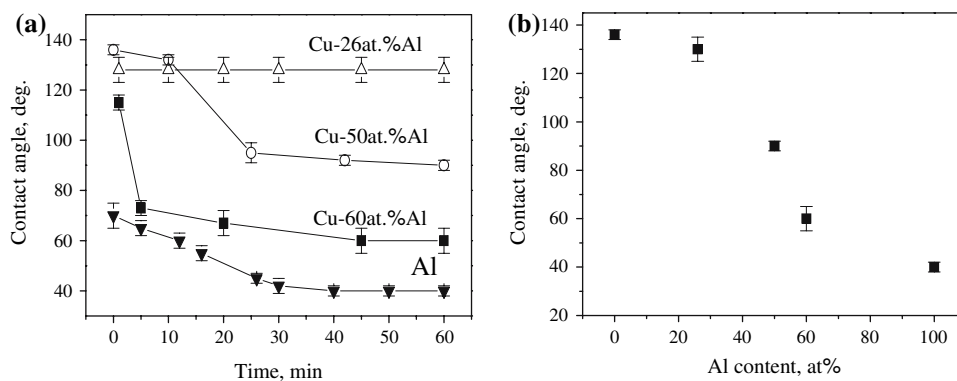


Fig. 2 Spreading kinetics of various Cu-Ti drops on the Er_2O_3 substrate (a) and final contact angles as a function of the melt composition after 60 min of contact at 1,423 K (b)

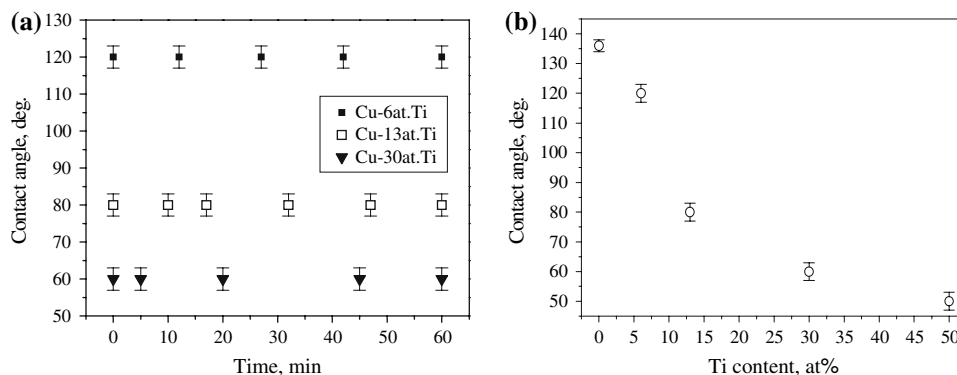


Fig. 3 Interface morphology in the $\text{Er}_2\text{O}_3/(\text{Cu}-\text{Al})$ system: (a) pure Al, (b) 60 at% Al, and (c) 50 at% Al

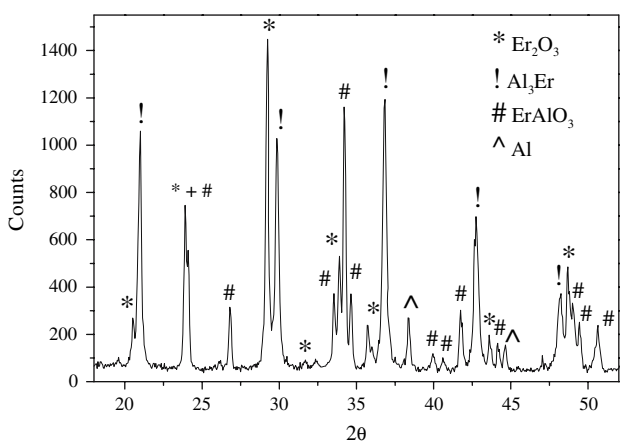
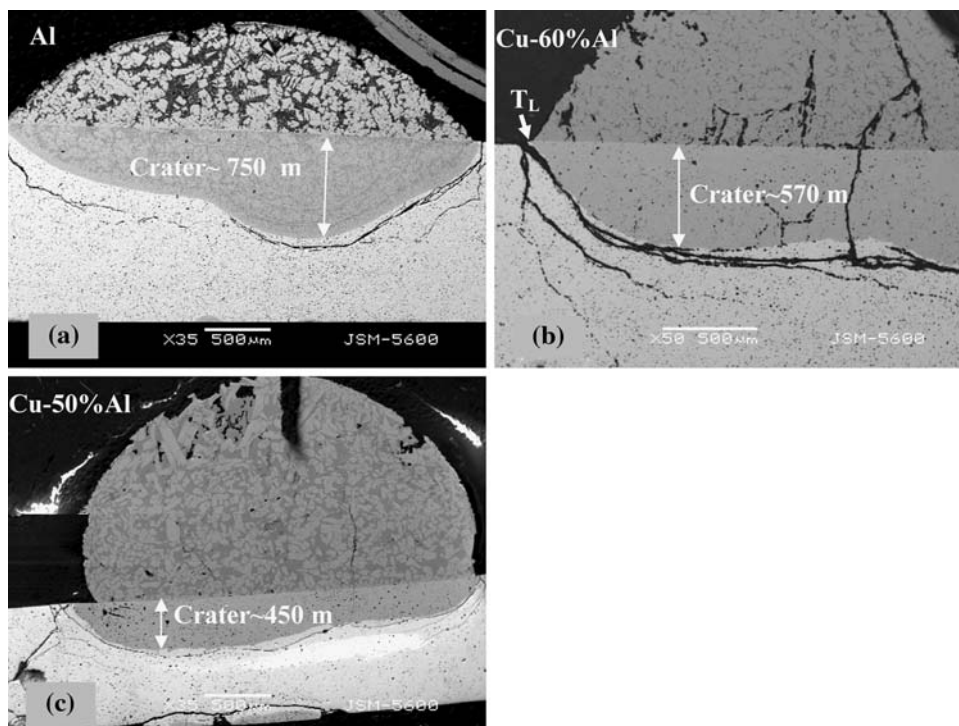


Fig. 4 XRD analysis results of the Al drop, detached from the Er_2O_3 substrate. The peaks of the residual Er_2O_3 from the substrate are also present

The crater has a composite structure, which consists of metal channels and the ErAlO_3 spinel.

The $\text{Er}_2\text{O}_3/(\text{Cu}-\text{Ti})$ interfaces

The metal drops in the $\text{Er}_2\text{O}_3/(\text{Cu}-\text{Ti})$ system were spontaneously detached from the Er_2O_3 substrates during cooling to room temperature. Cross sections of the detached drops, which include residua of the Er_2O_3 substrate, were examined by EDS and WDS analysis. Very thin (<1 μm) interfacial Ti-enriched layer (Fig. 6) was

detected. Quantitative EDS analysis using the Er_2O_3 as a standard indicates that the composition of this layer is close to the ErTiO_3 spinel phase. The presence of Ti and Er in the interfacial layer was confirmed by Auger depth profile performed on the surface of the detached drop, which was in contact with the substrate (Fig. 7).

Discussion

Previous investigation of the $\text{Y}_2\text{O}_3/(\text{Cu}-\text{Al})$ system [5] revealed that Al reacts with Y_2O_3 , forms YAlO_3 beneath the drop releasing Y, which dissolves in the melt. The interaction is accompanied with a relatively deep crater formation at the oxide/metal interface. It was established that the depth of the crater depends on the departure of the initial metal drop composition from the composition of the melt equilibrated with the Y_2O_3 and YAlO_3 phases. The experimental results were well accounted for by the thermodynamic analysis of the YAlO_3 phase formation. Similar interface evolution takes place in the $\text{Er}_2\text{O}_3/(\text{Cu}-\text{Al})$ and $\text{Er}_2\text{O}_3/(\text{Cu}-\text{Ti})$ systems. The interaction in the first system is significantly stronger and the crater is remarkably deeper than that in the second one. These experimental observations may be also accounted for by a thermodynamic analysis of the reactions, which take place in the systems.

The formation of the ErAlO_3 phase at the $\text{Er}_2\text{O}_3/(\text{Cu}-\text{Al})$ interface may be described by the chemical reaction (1):

Fig. 5 The microstructure of the $\text{Er}_2\text{O}_3/(\text{Cu}-50\text{at}\%\text{Al})$ interface after chemical etching. Overall view of the crater formed beneath the Cu–Al drop (a), the composite structure of the crater containing Cu–Al channels (gray areas) in the ErAlO_3 ceramic matrix (white areas). The dark spots may be attributed to intrinsic porosity or to metallic phase removed during sample preparation

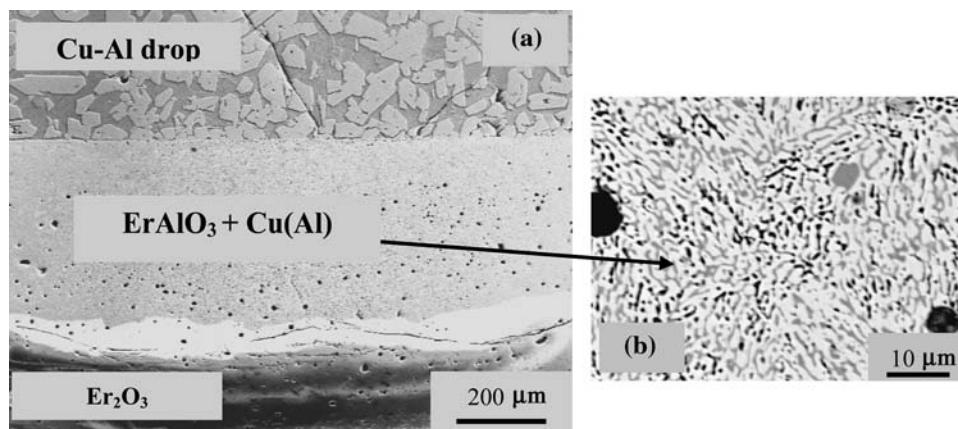


Fig. 6 Back scattered electrons image of the cross sectioned $\text{Er}_2\text{O}_3/\text{Cu}-20\text{at}\%\text{Ti}$ interface (a), WDS line scans of Ti and Cu across the interface (b)

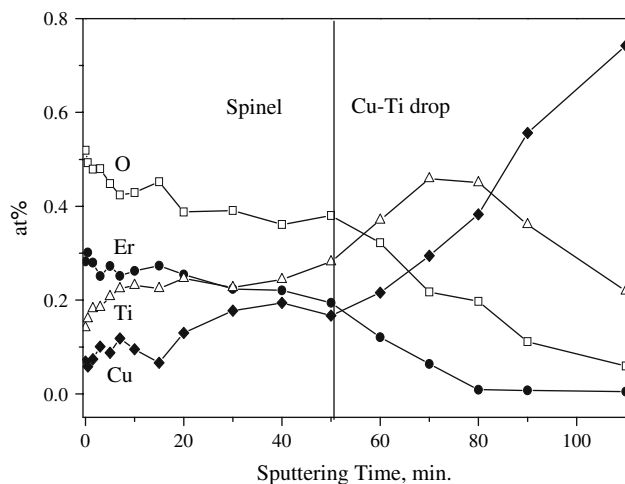
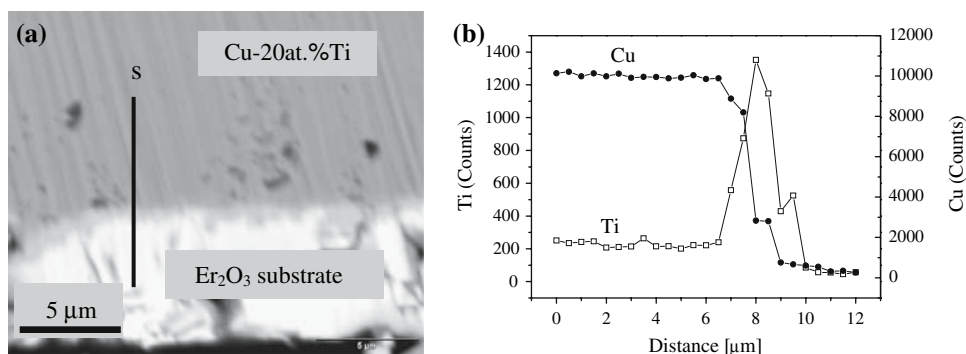


Fig. 7 Auger depth profile performed on the surface the detached Cu-20at%Ti drop



The underline indicates that Al and Er are in the liquid solution. Unfortunately, the standard Gibbs energy of ErAlO_3 formation is not readily accessible. In order to estimate the equilibrium constant (K) for reaction (1) at 1,423 K, it was assumed that the Gibbs energy $\Delta G_f^*(\text{ErAlO}_3)$ of the ErAlO_3 phase formation from pure Er_2O_3 and Al_2O_3 oxides is equal to $\Delta G_f^*(\text{YAlO}_3)$ for the

formation of YAlO_3 formed from pure Y_2O_3 and Al_2O_3 . According to data [7], the standard Gibbs energy for the YAlO_3 phase formation from pure elements $\Delta G_f^0(\text{YAlO}_3) = -1,390$ kJ/mol. Using the standard Gibbs energies for the oxides (Table 1) the value of $\Delta G_f^*(\text{YAlO}_3)$ was calculated as equal to -31 kJ/mol. The value of $\Delta G_f^0(\text{ErAlO}_3) = -1,386$ kJ/mol was estimated according to Eq. 2.

$$\Delta G_f^0(\text{ErAlO}_3) = \frac{\Delta G^0(\text{Er}_2\text{O}_3) + \Delta G^0(\text{Al}_2\text{O}_3)}{2} + \Delta G_f^*(\text{ErAlO}_3) \quad (2)$$

Using the estimated value of $\Delta G_f^0(\text{ErAlO}_3)$ and ΔG^0 of erbium melting ($\Delta H^0(\text{melting}) = 19,903$ kJ/mol and $T(\text{melting}) = 1,795$ K [8]), the equilibrium constant of Eq. 1 at 1,423 K was estimated as:

$$K(1) = \frac{a_{\text{Er}}}{a_{\text{Al}}} = \exp\left(\frac{-\Delta G^0(1)}{RT}\right) = 1.25 \times 10^{-4} \quad (3)$$

where a_{Er} and a_{Al} are the activities of Er and Al in the Cu–Al–Er liquid solution referred to pure Er and Al in the

Table 1 Standard formation Gibbs energies of Y, Er, Al and Ti oxides at 1,423 K [8]

Oxide	Al_2O_3	Y_2O_3	Er_2O_3	Ti_2O_3
ΔG_f^0 (kJ/mol)	-1221.50	-1496.58	-1487.82	-1131.26

liquid state. When the activities ratio (a_{Er}/a_{Al}) is less than 1.25×10^{-4} , the $ErAlO_3$ phase is formed and the released Er dissolves in the melt. The equilibrium constant is very sensitive to the Gibbs energy values and an error ± 10 kJ/mol of the $\Delta G_f^0(ErAlO_3)$ value leads to $K(1)$ variation from 5.4×10^{-5} to 2.9×10^{-4} . Thus, the results of the thermodynamic analysis should be considered qualitatively only.

In the $Er_2O_3/(Cu-Ti)$ system a very thin ($<1 \mu m$) interfacial ($ErTiO_3$) layer was observed. Thus, the reaction that takes place at the $Er_2O_3/(Cu-Ti)$ interface may be written as:



We have to point out again that thermodynamic properties of the $ErTiO_3$ phase are not available. The estimation of the standard Gibbs energy formation for the $ErTiO_3$ phase was performed according to the assumptions, which were taken into account for the $ErAlO_3$ phase formation (Eq. 3). In the case of $ErTiO_3$ it could be written:

$$\Delta G_f^0(ErTiO_3) \approx \frac{\Delta G^0(Ti_2O_3) + \Delta G^0(Er_2O_3)}{2} + \Delta G_f^*(ErTiO_3) \tag{5}$$

The formation Gibbs free energy $\Delta G_f^*(ErTiO_3)$ for $ErTiO_3$, formed from pure Er_2O_3 and Ti_2O_3 , is assumed to be equal to $\Delta G_f^*(YAlO_3)$ and therefore the estimated value of $\Delta G_f^0(ErTiO_3)$ is equal to $-1,341$ kJ/mol.

The standard Gibbs energy and the equilibrium constant of the reaction (4) were calculated as $\Delta G_f^0(4) = 137,324$ kJ/mol and $K(4) = \frac{a_{Er}}{a_{Ti}} = \exp\left(\frac{-\Delta G^0(5)}{RT}\right) = 3.8 \times 10^{-6}$, respectively. The activities of the component of liquid solution are referred to pure Er and Ti in the liquid state.

If the activities ratio (a_{Er}/a_{Ti}) is less than 3.8×10^{-6} the $ErTiO_3$ phase is formed and the released Er dissolves in the melt. It should be noted again that an error ± 10 kJ/mol of the $\Delta G_f^0(ErTiO_3)$ value leads to $K(4)$ variation from 1.6×10^{-6} to 8.9×10^{-6} .

In order to estimate the composition of liquid solutions, the thermodynamic properties of the melts have to be used. The thermodynamic activities of the components in the ternary solutions were estimated by using the Redlich–Kister approach [9] and the reported data for the binary solutions.

The activities of Al and Ti in the binary Cu–Al and Cu–Ti melts [10, 11] as a function of their composition are shown in Fig. 8. The Cu–Al liquid solution exhibits a strong negative departure from ideality, while the behavior of Cu–Ti liquid solution is close to ideal. The Redlich–Kister coefficients for these systems were derived and presented in Table 2. The Redlich–Kister coefficients for the binary Al–Er system (Table 2) were reported by

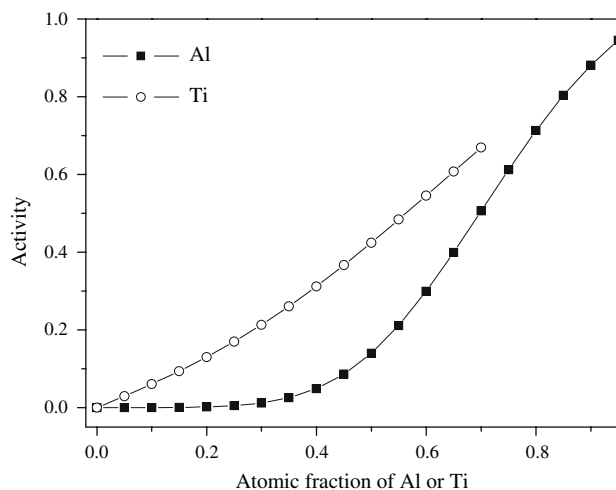


Fig. 8 The activities of Al and Ti in liquid Cu–Al and Cu–Ti binary melts at 1,423 K

Table 2 Redlich–Kister coefficients for the binary Er–Al, Cu–Al and Cu–Er melts at 1,423 K

R.K. coefficients (J/mol)	Er–Al [12]	Cu–Al [10]	Cu–Er [4]	Cu–Ti [11]	Er–Ti
0L	–97,246	–82,187	–92,000	–12,067	0
1L	–3,317	21,967	0	0	0
2L	22,630	0	0	0	0

Cacciamani et al. [12]. In order to estimate the 0L coefficient for Cu–Er system, the reported data [4] on the partial enthalpy ($-92,000$ J/mol) for dilute Cu–Er solution was used. According to the binary Er–Ti phase diagram [13], there are no stable intermetallic phases in this system and it was assumed that interatomic interaction is weak, thus the Er–Ti liquid solution, at least for the low Er content, may be considered as ideal.

The calculated erbium concentrations in the solutions that are in equilibrium with the ceramic phases are presented in Fig. 9. The Er content in the Cu–Ti–Er melt is extremely low (about 10^{-4} atomic fraction), while this value for Cu–Al–Er solution reaches a few atomic percents.

The results of the thermodynamic calculations are in a good agreement with the actual detected Er contents in the Cu–Al and Cu–Ti drops and emphasize the role of thermodynamic properties of liquid solutions on the wetting behavior. For the relatively high Al content in the melt (about 50 at%) its activity is yet low and is not sufficient for the formation of the $ErAlO_3$ spinel. Only at higher Al contents (above 50 at%) it is able to react with Er_2O_3 , and to release Er, which dissolves in the melt and stands behind the deep crater formation.

The $ErTiO_3$ phase is thermodynamically less stable compared to the $ErAlO_3$ phase and Ti dissolved in the melt,

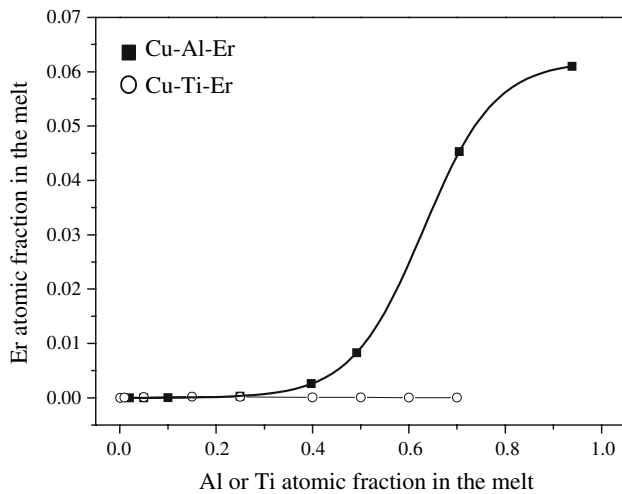


Fig. 9 The calculated equilibrium content of Er in Cu–Al and Cu–Ti alloys in contact with Er_2O_3 at 1,423 K according to Eqs. 1 and 4

which has relatively high activities, cannot react with Er_2O_3 and release Er. This is a reason of the formation of only thin interfacial layer in this system.

Conclusions

The interaction between Er_2O_3 substrate and liquid Cu alloyed by active elements (Ti and Al) was investigated. It was established that the Er_2O_3 substrate reacts with the active elements dissolved in liquid Cu and the formation of the ErAlO_3 and ErTiO_3 phases takes place. The released Er dissolves in the melt and a crater is formed at the interface. A deep crater (about 500 μm) was observed at the Er_2O_3 /(Cu–Al) interface, while the depth of the reaction region at the Er_2O_3 /(Cu–Ti) interface was extremely low (<1 μm). The spreading kinetics and the final contact angle in these

systems are controlled by the formation of the interfacial spinel layer. The experimental observations are in a good agreement with the thermodynamic analysis, which emphasizes the dominance of the thermodynamic properties of the melt in the wetting behavior of the Er_2O_3 substrate by liquid Cu containing Al and Ti as active additives.

Acknowledgement This work was supported by a grant from the Israeli Council of High Education and the Israeli Atomic Energy Commission.

References

1. Harter I, Dusserre P, Duffar T, Nabot JP, Eustathopoulos N (1993) *J Cryst Growth* 131:157
2. McDeavitt SM, Billings GW, Indacochea JE (2002) *J Mater Sci* 37:3765
3. Indacochea JE, Billings GW, McDeavitt SM (2005) *Ceram Trans* 146:103
4. Naidich YuV, Zhuravlev VS, Frumina NI (1990) *J Mater Sci* 25:1895
5. Barzilai S, Aizenshtein M, Froumin N, Frage N (2006) *J Mater Sci* 41:5108
6. Froumin N, Frage N, Polak M, Dariel MP (1997) *Scripta Mater* 37:1263
7. Fabrichnaya O, Seifert HJ, Weiland R, Ludwig T, Aldinger F, Navrotsky A (2001) *Z Metallkd* 92:1083
8. SGTE substances database, SSUB3, version 3.1, 2001/2002
9. Hillert M (1988) *Phase equilibria, phase diagram and phase transformation – their thermodynamic basis*, 1st edn. Cambridge University Press
10. Ansara I, Dinsdale AT, Rand MH (1998) *Cost 507 – thermochemical database for light metal alloys, V. 2*, European Communities, Belgium
11. Wei P, Jie L (1999) *Mat Sci Eng A Struct* 269:104
12. Cacciamani G, Saccone A, DE negri S, Ferro R (2002) *J Phase Equil* 23:38
13. Er-Ti phase diagram (1996), *Binary alloy phase diagrams* 2nd edition Plus, ASM International, The Materials Information Society